

Mechanisms for Li and Be production in the $^{14}\text{N} + ^{12}\text{C}$ reaction*

R. G. Stokstad

Oak Ridge National Laboratory, Oak Ridge, Tennessee 37830

M. N. Namboodiri, E. T. Chulick,[†] and J. B. Natowitz

Department of Chemistry and Cyclotron Institute, Texas A & M University, College Station, Texas 77843

D. L. Hanson[†]

Wright Nuclear Structure Laboratory, Yale University, New Haven, Connecticut 06520

(Received 23 May 1977)

Measurements of the yields of ^6Li and ^7Be have been made for the $^{14}\text{N} + ^{12}\text{C}$ reaction at $E_{^{14}\text{N}} = 86.9$ and 157.0 MeV. Statistical model calculations are compared with the data in order to determine the reaction mechanism. It is concluded that more than half of the total Li and Be yield at these bombarding energies arises from processes other than compound nucleus formation and the subsequent evaporation of a ^6Li or ^7Be nucleus. The most likely production mechanism at high bombarding energies appears to be the decay of a projectile-like fragment excited in a peripheral collision.

[NUCLEAR REACTIONS $^{12}\text{C}(^{14}\text{N}, ^6\text{Li})$, $^{12}\text{C}(^{14}\text{N}, ^7\text{Be})$, $E = 86.9$ and 157.0 MeV; measured $\sigma(E, \theta)$; compared with statistical model calculations.]

I. INTRODUCTION

The production of lithium and beryllium in heavy-ion reactions such as $^{14}\text{N} + ^{12}\text{C}$ has been of interest for several reasons. Since the masses of these nuclei do not differ greatly from those of the projectile or target, direct multinucleon transfer has been considered as a possible reaction mechanism.¹ The evaporation of ^7Be by the ^{26}Al compound nucleus and its possible production via a fission process were investigated by Holub *et al.*² They found that these mechanisms were unable to account for their measured total yields of ^7Be . An important step in the understanding of the reaction mechanism was the observation³ of symmetry about 90° c.m. in the angular distribution for the $^{12}\text{C}(^{14}\text{N}, ^6\text{Li})^{20}\text{Ne}$ reaction populating discrete states in ^{20}Ne . These measurements²⁻⁴ and quantitative Hauser-Feshbach analyses⁵ of the absolute cross sections showed that compound-nucleus formation was the dominant mechanism for producing ^6Li and ^7Be nuclei in the $^{14}\text{N} + ^{12}\text{C}$ reaction, at least for moderate bombarding energies. It was found⁵ that an angular-momentum cutoff was required in order to reproduce the measured yields with the statistical model, and that this critical angular momentum at $E_{\text{c.m.}} = 36$ MeV was consistent with expectations based on entrance-channel models⁶ or estimates of the location of the yrast line of the compound nucleus.⁷ This demonstrated the possibility of using reactions such as $^{12}\text{C}(^{14}\text{N}, ^6\text{Li})^{20}\text{Ne}$ to measure the critical angular momentum for fusion and, thereby, to study the entrance-channel dynamics of the reaction and the properties of the compound nucleus.

A large amount of work toward this end has been done since then using different methods. Volant *et al.*⁸ have measured and analyzed the cross sections for $^{12}\text{C}(^{14}\text{N}, ^6\text{Li})^{20}\text{Ne}$ to discrete low-lying states over the bombarding energy range 9–28 MeV c.m. Klapdor, Reiß, and Rosner⁹ have made comparisons of the statistical model to data^{1,3,10} taken over the energy range 9–55 MeV c.m. and have suggested an analysis of the shape of the ^6Li evaporation spectrum and of the ratios of cross sections to different discrete states in order to determine the critical angular momentum.

The deduction of a critical angular momentum, J_c , or other information from the measured yields by the above methods requires that two criteria be fulfilled. The statistical model and the parameters incorporated in it must be reliable, and the quantity being analyzed must be the result of a statistical or compound-nuclear process.

That the first of these criteria is met has been shown by numerous comparisons of statistical model calculations with experimental data at relatively low bombarding energies¹⁰⁻¹² where the effects of a critical angular momentum are relatively small and the reactions are known⁷ to proceed via compound-nucleus formation and decay.

The second of these criteria is the subject of the present work. At high bombarding energies, e.g., above 36 MeV c.m., the differential cross sections for the population of individual low-lying states drop rapidly, measurements of J_c by analysis of these cross sections become impossible, and total yields must be analyzed. The total yields of Li and Be from reactions such as $^{12}\text{C} + ^{14}\text{N}$ and $^{10}\text{B} + ^{16}\text{O}$ ap-

TABLE I. Angle-integrated yields of ${}^6\text{Li}$ and ${}^7\text{Be}$ produced at low bombarding energies.

Reaction	E_{lab} (MeV)	Experimental yield (mb)	Hauser-Feshbach ^a (mb)
${}^{12}\text{C}({}^{14}\text{N}, {}^6\text{Li}){}^{20}\text{Ne}$ ^b	25.0	0.39 ± 0.04	0.48
	30.0	0.89 ± 0.09	0.98
	36.0	1.35 ± 0.14	1.70
${}^{10}\text{B}({}^{16}\text{O}, {}^6\text{Li}){}^{20}\text{Ne}$ ^b	19.5	0.18 ± 0.02	0.13
	24.3	0.37 ± 0.04	0.41
	31.5	1.05 ± 0.10	0.90
${}^{12}\text{C}({}^{14}\text{N}, {}^7\text{Be}){}^{19}\text{F}$ ^c	35	0.025 ± 0.015 ^d	0.006 ^d
	42	0.15 ± 0.07	0.15
	49	0.35 ± 0.15	0.80
	54	2.0 ± 0.8	2.2
	59	3.7 ± 1.4	3.7

^a As described in Refs. 5 and 12.

^b Reference 12.

^c Reference 4.

^d Thick target yields; the units here are $\text{mb} \times \text{mg}/\text{cm}^2$.

pear to be compound in nature at bombarding energies up to ~ 30 MeV c.m. as shown in Table I. The compound nature of the reaction mechanism at higher bombarding energies needs to be established through a detailed comparison of statistical model predictions with the data. This comparison is facilitated by recent measurements of fusion cross sections in which evaporation residues are detected and a critical angular momentum is deduced independent of a statistical model.¹³⁻¹⁵ We present here measurements of the ${}^6,7\text{Li}$ and ${}^7,9\text{Be}$ yields for the ${}^{14}\text{N} + {}^{12}\text{C}$ reactions at $E_{14\text{N}} = 86.9$ and 157 MeV. Statistical model calculations¹⁶ for both first- and second-chance emission are compared with the experimental data.

II. EXPERIMENT AND RESULTS

Beams of ${}^{14}\text{N}$ at energies of 86.9 and 157 MeV from the variable energy cyclotron at Texas A & M University were used to bombard a natural carbon target. The thickness of the target, $228 \pm 16 \mu\text{g}/\text{cm}^2$, was determined by weighing. The uniformity of similar targets was found to be typically $\pm 5\%$. The reaction products were recorded simultaneously at two angles by two independent semiconductor telescopes, each having a $50 \mu\text{m}$ ΔE detector and a 2 mm E detector. In a later experiment, a three-element telescope having detectors of $8.4 \mu\text{m}$, $36 \mu\text{m}$, and 1 mm thickness was used. The data were recorded event by event on magnetic tape using an IBM-7094 computer and analyzed off line. The particle identification scheme described by Chulick, Natowitz, and Schnatterly¹⁷ was used and enabled isotopic resolution of nuclei up to mass 12. This is illustrated in Fig. 1. The error on the

absolute differential cross sections arising from uncertainties in the target thickness, the beam current integration, and detector solid angle is $\pm 10\%$.

A typical energy spectrum of ${}^6\text{Li}$ ions is shown in Fig. 2. The dashed line indicates the extrapolation of the spectrum to energies below the minimum ${}^6\text{Li}$ energy required to pass through the ΔE detector. The scale at the top gives the excitation energy in ${}^{20}\text{Ne}$ assuming two-body reaction kinematics.

The angular distributions for energy-integrated yields of ${}^6,7\text{Li}$ and ${}^7,9\text{Be}$ are shown in Fig. 3 for $E_{14\text{N}} = 86.9$ MeV. The data indicate an exponential

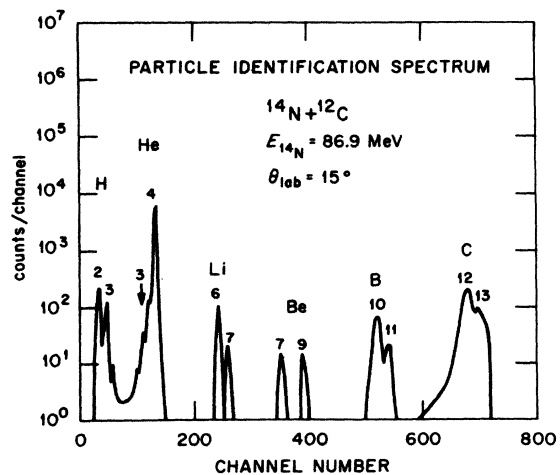


FIG. 1. The particle identification spectrum illustrating the isotopic resolution attained for particles up to mass 12.

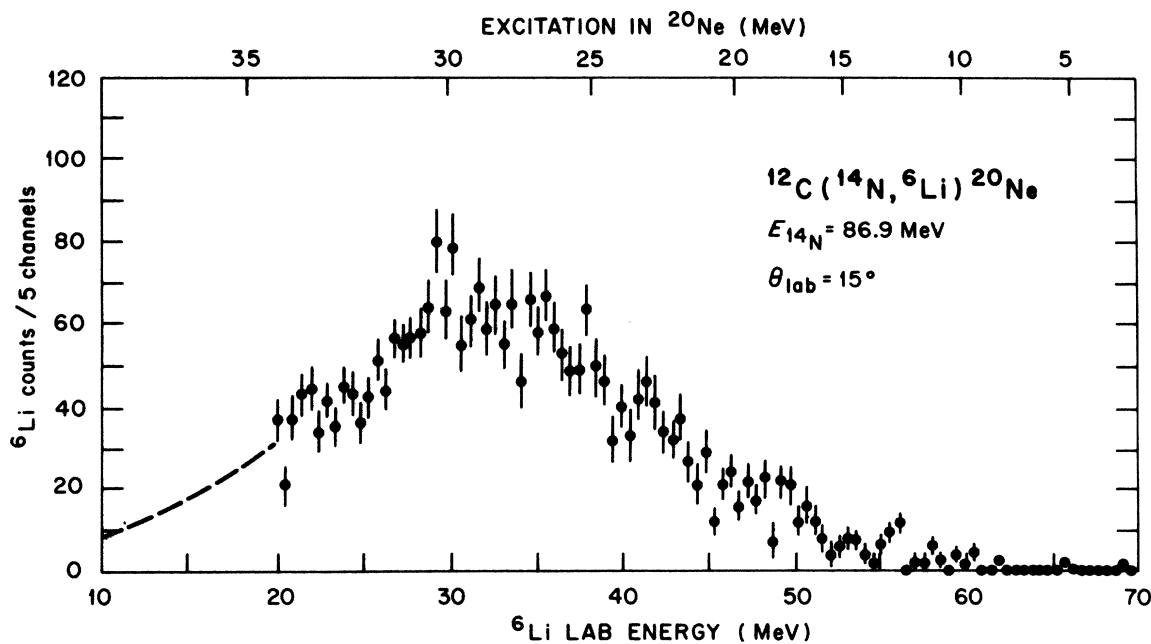


FIG. 2. A typical spectrum of ${}^6\text{Li}$ ions. The scale at the top indicates the excitation energy in ${}^{20}\text{Ne}$ calculated with two-body kinematics for the reaction ${}^{12}\text{C}({}^{14}\text{N}, {}^6\text{Li}){}^{20}\text{Ne}$. The dashed line shows the extrapolation made for particles stopped in the ΔE detector.

dependence on the scattering angle. The straight lines on the semilog plots of Fig. 3 correspond to $(d\sigma/d\Omega)_{\text{lab}} = N e^{-k\theta_{\text{lab}}}$ where N (mb) and k (deg^{-1}) for ${}^6\text{Li}$, ${}^7\text{Li}$, ${}^7\text{Be}$, and ${}^9\text{Be}$ are (29.0, 0.045), (6.9, 0.049), (5.8, 0.046), and (7.8, 0.048), respectively.

The angle-integrated yields obtained at both bombarding energies are given in Table II along with results obtained at comparable bombarding energies at Oak Ridge¹⁴ and at Berkeley.¹⁵ The present values are larger than the preliminary values cited in Ref. 7 and are the result of an improved measurement of the yield of those Li and Be nuclei emerging with low energies.

III. STATISTICAL MODEL CALCULATIONS AND COMPARISON WITH THE DATA

Cross sections for compound-nucleus formation and decay were calculated with the Hauser-Fesh-

bach expression¹⁸ and the computer code STATIS.¹⁹ These calculations, including the optical-model and level-density parameters employed, are described in detail in Ref. 5. Figure 4 illustrates the sensitivity of the partial Li and Be yields to the total angular momentum of the compound nucleus at a bombarding energy of $E_{14\text{N}} = 78$ MeV ($E_{\text{c.m.}} = 36$ MeV). The partial cross section σ_J for angular momentum J increases with J much more rapidly for the energetically unfavored, heavier particles of mass 6 and mass 7 than it does for protons or α particles.

Although there is a high sensitivity to the particular value of the maximum angular momentum in the cutoff region, the total cross sections for ${}^6\text{Li}$ and ${}^7\text{Be}$ production, as shown in Fig. 4, constitute only a small portion of the total cross section for compound-nucleus formation.

The predicted cross sections for ${}^6, {}^7\text{Li}$ and ${}^7, {}^9\text{Be}$

TABLE II. Total yields of ${}^6, {}^7\text{Li}$ and ${}^7, {}^9\text{Be}$ produced in the ${}^{14}\text{N} + {}^{12}\text{C}$ reaction, in mb.

$E_{14\text{N}}$	${}^6\text{Li}$	${}^7\text{Li}$	${}^6\text{Li} + {}^7\text{Li}$	${}^7\text{Be}$	${}^9\text{Be}$	${}^7\text{Be} + {}^9\text{Be}$	Ref.
86.9	22.8 ± 2.3	4.3 ± 0.5	27.1 ± 2.4	4.3 ± 0.7	5.3 ± 0.8	9.6 ± 1.1	Present work
86.3 ^a			29.0 ± 3.5			8.8 ± 1.1	14
157.4	76 ± 9	38 ± 5	114 ± 10	21.5 ± 3	21.5 ± 3	43.0 ± 4	Present work
158.0 ^a			105 ± 10			49 ± 5	15

^a The Li and Be isotopes were not separated in these measurements and should be compared with the sum of the corresponding isotopic yields in the present work.

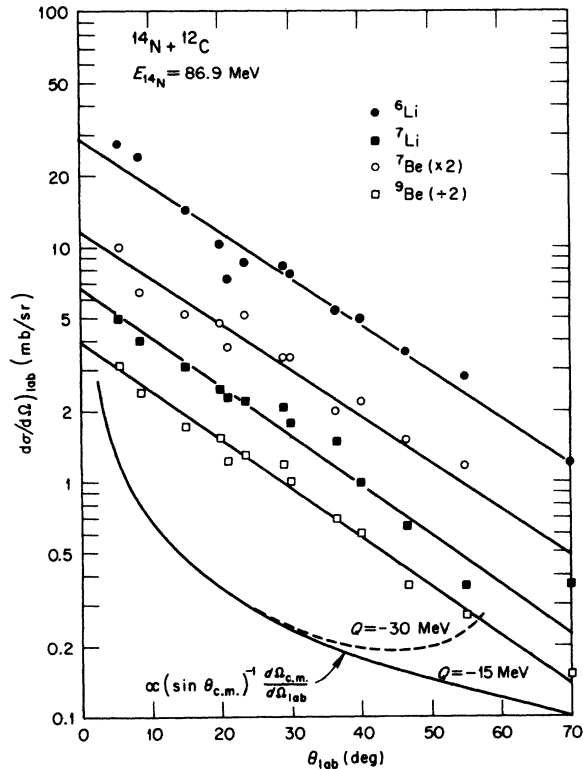


FIG. 3. Angular distributions for the energy-integrated yields of ${}^6,{}^7\text{Li}$ and ${}^7,{}^9\text{Be}$. The yield at each angle has been corrected for particles which stop in the ΔE detector, as shown in Fig. 1. For clarity, the measured cross section for ${}^7\text{Be}$ has been multiplied by 2 before plotting. The actual cross sections at 5.5° lab for ${}^7\text{Be}$ and ${}^9\text{Be}$ are 5.0 and 6.5 mb, respectively. The solid and dashed curves in the lower part of the figure are normalized laboratory system cross sections for the ${}^{12}\text{C}({}^{14}\text{N}, {}^6\text{Li}){}^{20}\text{Ne}$ reaction at Q values of -15 and -30 MeV, respectively. The angular distribution in the center-of-mass system is $(\sin\theta_{c.m.})^{-1}$.

production are shown in Fig. 5 as a function of the maximum or cutoff angular momentum J_c for a bombarding energy of 86.9 MeV ($E_{c.m.} = 40.1$ MeV). The value of the ${}^{12}\text{C} + {}^{14}\text{N}$ transmission coefficient T_l for $l = J_c$ is also indicated in this figure. A total of 17 types of particle exit channels were used in calculating the denominator of the Hauser-Feshbach formula. This decreases the predicted yields by 8% compared with a six-channel calculation including only p , n , d , α , ${}^6\text{Li}$, and ${}^{12}\text{C}$ emission. The sensitivity of the predicted cross sections to a variation in the moment of inertia in the level density formula is much smaller for energy-integrated total yields than it is for the cross section to, e.g., a specific low-lying state in ${}^{20}\text{Ne}$. If the radius parameter r_0 used to compute the rigid-body moment of inertia is changed from 1.5 fm (the value used) to 1.4 fm the predicted total yields in-

crease by only 30%. Only first-chance emission is included in the prediction shown in Fig. 5; the effect of second-chance emission will be considered in the discussion following.

If the entire experimental yields of ${}^6\text{Li}$ and ${}^7\text{Be}$ and ${}^9\text{Be}$ production are to be accounted for by compound-nucleus formation and Li or Be evaporation, then nearly the entire reaction cross section, including partial waves up to the grazing value $l_g \sim 23\hbar$, would have to go into compound-nucleus formation. The yield of ${}^7\text{Li}$ is a factor of 2 larger than the predicted compound yield for any cutoff angular momentum. On the other hand, the value of the critical angular momentum for compound-nucleus formation in the ${}^{12}\text{C} + {}^{14}\text{N}$ reaction has been determined from measurements of the fusion cross section in which the evaporation residues are detected.^{14,15} These critical angular momenta are shown in Fig. 6 as a function of excitation energy in ${}^{26}\text{Al}$, the latter being defined as the c.m. bombarding energy plus the ${}^{12}\text{C} + {}^{14}\text{N}$ separation energy of 15 MeV. The measured value¹⁴ of J_c at $E_{14\text{N}}$

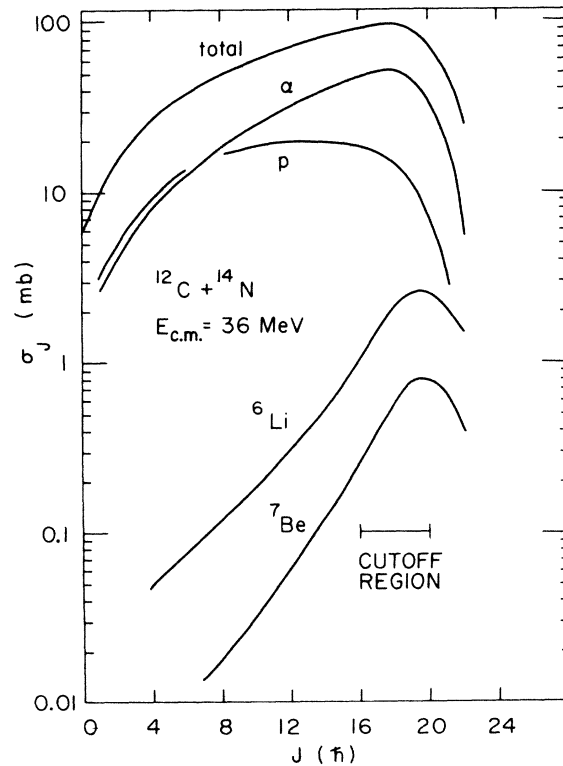


FIG. 4. Predicted angle-integrated yields for light particles emitted in the formation of a compound nucleus by the ${}^{14}\text{N} + {}^{12}\text{C}$ reaction at $E_{14\text{N}} = 36$ MeV, c.m. The partial cross section for angular momentum J is given. The total compound cross section σ is given by $\sum_{J=0}^{J_c} \sigma_J$ where J_c is the angular momentum cutoff.

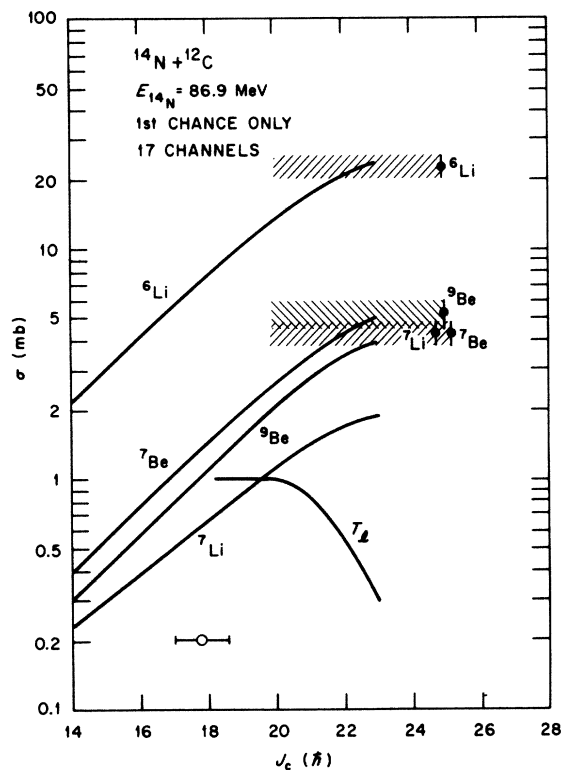


FIG. 5. Predicted compound-nuclear cross sections in mb for ^6Li and $^7,^9\text{Be}$ production at $E_{^{14}\text{N}} = 86.9$ MeV as a function of the cutoff angular momentum J_c . The transmission coefficient in the entrance channel for $l = J_c$ is also shown (in which case the ordinate is in units of \hbar). The experimental yields in mb are shown as shaded horizontal bands with the exact values given by the solid points. The value of the cutoff angular momentum deduced from evaporation residue measurements (Ref. 14) is shown as an open circle.

$= 86.3$ MeV is $(17.8 \pm 0.8)\hbar$ and is also shown in Fig. 5. Using this value for J_c in the Hauser-Feshbach calculations results in a predicted first-chance ^6Li yield of 7 ± 2 mb, suggesting that only one third of the measured yield arises from a compound process (see Fig. 5). The situation for ^7Be and ^9Be is similar, while for ^7Li $\sim 15\%$ of the measured yield appears to arise from a compound process.

A similar situation is encountered at 157 MeV bombarding energy, as shown in Fig. 7. A cutoff angular momentum equal to a larger than grazing angular momentum would be required in order to account for the measured yields solely on the basis of compound-nucleus formation and decay. Using the value of J_c (25.7 ± 1.0) \hbar obtained from evaporation residue measurements¹⁵ indicates that compound-nucleus formation and first-chance decay account for approximately 39%, 15%, 36%, and 22% of the measured ^6Li , ^7Li , ^7Be , and ^9Be yields, re-

spectively.

Calculations of the cross sections for second-chance emission of Li and Be nuclei (an evaporation occurring after another particle such as a proton, neutron, or α particle has already been emitted) were made with the computer code BREAK-UP.¹⁶ These results are given in Table III along with those of first-chance calculations made under the same conditions. This type of calculation has been described in Ref. 11. Table III indicates that the cross section for the emission of a ^6Li nucleus after one particle has been emitted (whether it be a proton, neutron, or α particle) is about 30% of the combined cross sections for first-chance and second-chance emission. In obtaining estimates for second-chance emission for cases not given in Table III, we have assumed that the cross section for second-chance emission varies with J_c in the same proportion as the first-chance emission. Similarly, we assume that the ratios of second-chance emission to the first emission of a p , n , or α particle are the same at $E_{c.m.} = 72.5$ and 40.1 MeV.

The comparison of predicted and measured total yields is summarized in Fig. 8. The statistical

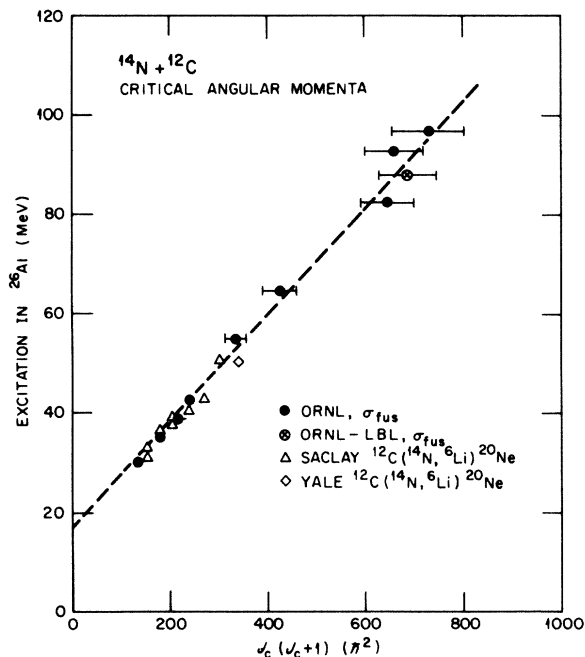


FIG. 6. Measured critical angular momenta, J_c , as a function of excitation energy in ^{26}Al . The latter quantity is given by $E_{c.m.} + 15$ MeV. The data points shown as circles are the results of evaporation residue measurements (Refs. 14 and 15). The other points are from statistical model analyses of the reaction $^{12}\text{C}(^{14}\text{N}, ^6\text{Li})^{20}\text{Ne}$ populating low-lying states in ^{20}Ne (Refs. 5 and 8).

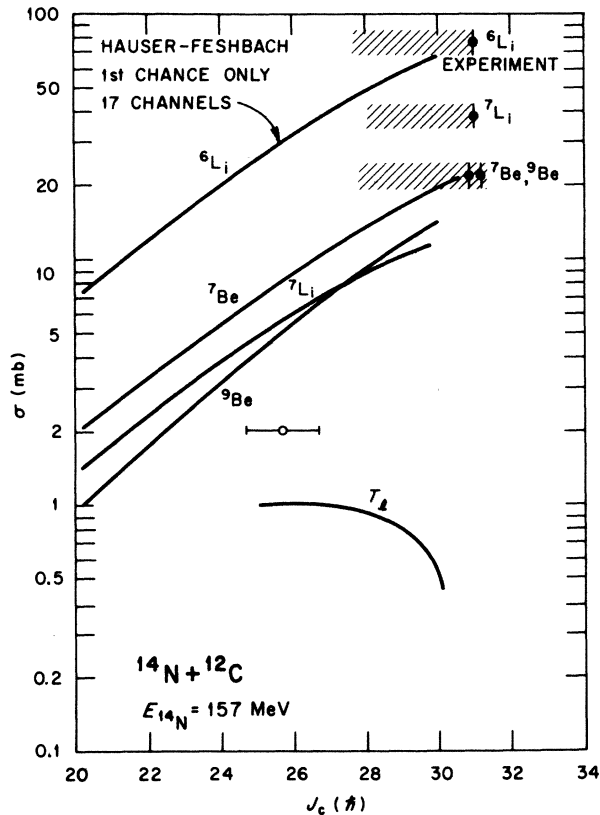


FIG. 7. Predicted compound-nuclear cross sections in mb for ${}^6,{}^7\text{Li}$ and ${}^7,{}^9\text{Be}$ production at $E_{14\text{N}} = 157$ MeV as a function of the cutoff angular momentum J_c . The transmission coefficient in the entrance channel for $l = J_c$ is also shown (in which case the ordinate is in units of \hbar). The experimental yields are shown as shaded horizontal bands with the exact values given by the solid points. The value of the cutoff angular momentum deduced from evaporation residue measurements (Refs. 14 and 15) is shown as an open circle.

model calculations have been made using the independently measured^{14,15} values for the critical angular momentum. We conclude from Fig. 8 that evaporation of a Li or Be nucleus by the excited compound nucleus cannot account for more (and is usually less) than half of the measured yields at ${}^{14}\text{N}$ bombarding energies between 86.9 and 157 MeV.

Other features of the experimental data to which the statistical model may be compared include the angular and energy distributions. The angular distributions for decay (by any process) of an equilibrated, rotating compound nucleus are well approximated by a $(\sin\theta_{\text{c.m.}})^{-1}$ dependence on the center-of-mass angle. A qualitative comparison of this prediction with energy-integrated yields given in the laboratory system may be made by transforming the $(\sin\theta_{\text{c.m.}})^{-1}$ angular distribution to the lab-

oratory system for various reaction Q values. Such distributions are shown unnormalized in Fig. 3 for ${}^{12}\text{C}({}^{14}\text{N}, {}^6\text{Li}){}^{20}\text{Ne}$ at $E_{14\text{N}} \sim 86.9$ MeV and for Q values of -15 and -30 MeV ($Q_{\text{g.s.}} = -4.2$ MeV). These angular distributions for compound-nucleus appear quite different from the exponential dependencies which reproduce the data for the energy-integrated yields at each angle. The angular distributions measured for discrete transitions to low-lying states in ${}^{20}\text{Ne}$ at $E_{14\text{N}} = 76$ MeV, however, do show a $(\sin\theta_{\text{c.m.}})^{-1}$ angular distribution³ which suggests that the departure from statistical behavior occurs with the lower energy portion of the ${}^6\text{Li}$ yield.

The energy dependence of the ${}^6\text{Li}$ yield observed at a fixed bombarding energy may be calculated using the Hauser-Feshbach formula and a level-density formula for the distribution of final states in ${}^{20}\text{Ne}$ (in exactly the same manner as the energy integral of this quantity is calculated for inclusion in the denominator of the Hauser-Feshbach formula). Until recently, the only data available for such a comparison were the spectra of Belote *et al.*³ obtained at $E_{14\text{N}} = 76.1$ and 120 MeV and at

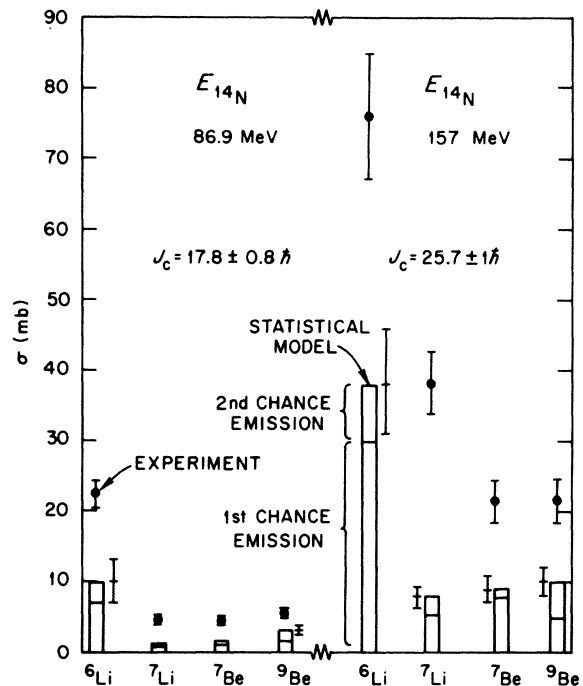


FIG. 8. Summary of the predicted total yields for ${}^6,{}^7\text{Li}$ and ${}^7,{}^9\text{Be}$ incorporating the critical angular momenta from evaporation residue measurements and including first- and second-chance emission. The error on the predicted yield arising from the uncertainty in the experimental value of J_c is indicated. The experimental yields are shown as solid points.

TABLE III. Statistical model calculations for two-step decay of ^{26}Al formed by $^{14}\text{N} + ^{12}\text{C}$.

$E_{\text{c.m.}}$ (MeV)	J_c (\hbar)	1st particle	2nd particle	Two-step angle-integrated cross section (mb)	One-step angle-integrated cross section ^a (mb)				
36.0	18	α	^6Li	2.6	7.5				
40.1	19	p	^6Li	1.2	4.4	10			
		n	^6Li	0.4					
		α	^6Li	2.8					
		p	^7Li	0.52	0.84		0.85		
		n	^7Li	0.17					
		α	^7Li	0.15					
		p	^7Be	0.12	0.43			1.9	
		n	^7Be	0.04					
		α	^7Be	0.27					
		p	^9Be	1.21	1.7				1.5
		n	^9Be	0.20					
		α	^9Be	0.32					
72.5	23	p	α	71	204	414			
		α	α	133					
72.5	23	α	^6Li	2.6	15.4				

^a The cross section for first-chance emission of the particle listed in column 4.

$\theta_{\text{lab}} = 10^\circ$ and 7° , respectively. Calculations of the energy spectra of ^6Li ions were made for these data and are shown in Figs. 9 and 10. Unfortunately, an absolute normalization for these early experimental data was not given³ and a comparison here may be made only with the shape of the spectrum. It may be seen that the predicted shapes for a wide range of cutoff angular momenta can fit the data in the high energy portion of the spectrum. However, at low ^6Li energies, all the predictions deviate from the data, especially those shown in Fig. 10.

Calculations of the double differential cross section $d^2\sigma/(d\Omega dE)$ for the reaction $^{12}\text{C}(^{14}\text{N}, \alpha)-^{22}\text{Na}(^6\text{Li})^{16}\text{O}$ were made with the computer codes¹⁶ BREAKUP and SEQUEL in order to check the possibility that ^6Li nuclei emitted on a second chance might be sufficiently low in energy and forward peaked to account for the observed yield in the low energy portion of the spectra shown in Figs. 9 and 10. The results are shown, along with the first-chance calculations, in Figs. 9 and 10. We conclude that second-chance emission is not the origin of the discrepancy between the experimental energy spectrum and the first-chance statistical model prediction.

A more meaningful comparison of the statistical model to the data is possible when the energy spectra are normalized. The ^6Li yield measured in the present work is shown in Fig. 11 as a function of

the ^6Li energy in the center-of-mass system. This spectrum was obtained by transforming a spectrum at a given lab angle, $d^2\sigma/(d\Omega_{\text{lab}} dE_{\text{lab}})$ to a center-of-mass energy scale, $d^2\sigma/(d\Omega_{\text{cm}} dE_{\text{c.m.}})$ and then integrating over the laboratory scattering angle. In this process, it is assumed that the entire yield is from the reaction $^{12}\text{C}(^{14}\text{N}, ^6\text{Li})^{20}\text{Ne}$, i.e. from a two-body reaction. The predicted cross sections for $J_c = 19\hbar$ or $20\hbar$ each can account for some portion of the ^6Li yield at high energies. The curve for $J_c = 18$ (the value of J_c given by evaporation residue measurements^{14,15}), however, does not reproduce the data at all. The major discrepancy is seen to occur at low ^6Li energies.

IV. DISCUSSION

The foregoing comparison of statistical model predictions to the experimental data shows that the major portion of the total $^6,^7\text{Li}$ and $^7,^9\text{Be}$ yields produced at bombarding energies greater than $E_{^{14}\text{N}} = 86$ MeV arises from processes other than compound-nucleus formation. At lower bombarding energies, however, the angle-integrated yields of ^6Li and ^7Be are well explained by evaporation of these particles from a compound nucleus (see Table I).

Thus one is led to consider other possible reaction mechanisms which could become important at high bombarding energies. At sufficiently high

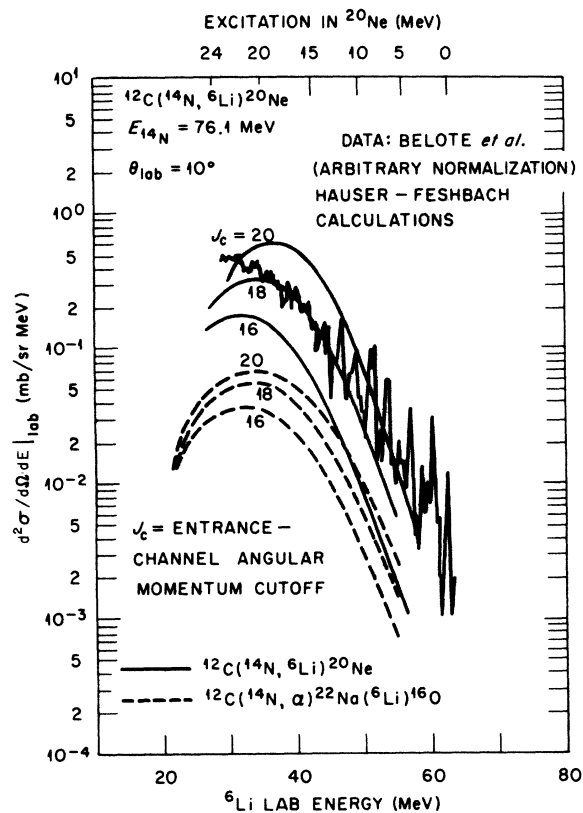


FIG. 9. Measured (Ref. 3) and predicted energy spectra for the yield of ${}^6\text{Li}$ ions produced in the ${}^{14}\text{N} + {}^{12}\text{C}$ reaction at $E_{14\text{N}} = 76.1$ MeV and $\theta_{\text{lab}} = 10^\circ$. The normalization of the experimental data (Ref. 3) is arbitrary; that of the calculations is absolute. The cross section for second-chance emission of a ${}^6\text{Li}$ ion following evaporation of an α particle is shown. The structure in the experimental spectrum corresponds to states (or groups of states) in ${}^{20}\text{Ne}$.

bombarding energies, the compound nucleus may have enough excitation energy to evaporate five α particles, leaving a ${}^6\text{Li}$ nucleus as an evaporation residue. The threshold for this process may be estimated by adding to the separation energy (23.4 MeV) the energy required to surmount the Coulomb and centrifugal barriers (42 MeV). The effective threshold is thus ~ 65 MeV c.m. or $E_{14\text{N}} \approx 140$ MeV. The amount of Li and Be residues which would be produced at $E_{14\text{N}} = 158$ MeV has been estimated with the computer code LILITA^{20,14} to be 18 and 4 mb for ${}^6\text{Li}$ and ${}^9\text{Be}$, respectively, with the amounts of ${}^7\text{Li}$ and ${}^7\text{Be}$ being negligible. Thus, production of Li and Be nuclei as evaporation residues is not able to account for the major portion of the Li and Be yields although its contribution at $E_{14\text{N}} = 157$ MeV is not entirely negligible.

Another process by which Li and Be nuclei may be produced is through the excitation of the projec-

tile to a state above the threshold for particle decay to Li or Be. The threshold for ${}^{14}\text{N}$ to decay to ${}^6\text{Li} + 2\alpha$ is only 16 MeV. Since this process is a direct-reaction mechanism involving peripheral collisions²¹ and not necessarily involving multinucleon transfer, the production cross sections could be quite large compared with those calculated for the evaporation of ${}^6\text{Li}$ from a compound nucleus. The laboratory energy of a ${}^6\text{Li}$ nucleus produced by this process may be roughly estimated as follows. The energy of a 86.9 MeV ${}^{14}\text{N}$ ion inelastically scattered at 15° lab and with 18 MeV of excitation is ~ 60 MeV. When this scattered nucleus decays, the emitted ${}^6\text{Li}$ ion would have, on the average, $\sim \frac{6}{14}$ of the energy of the ${}^{14}\text{N}^*$ ion or about 26 MeV. Thus these particles would appear in the low energy portion of the spectrum shown in Fig. 2. This is also the region where the statistical model grossly un-

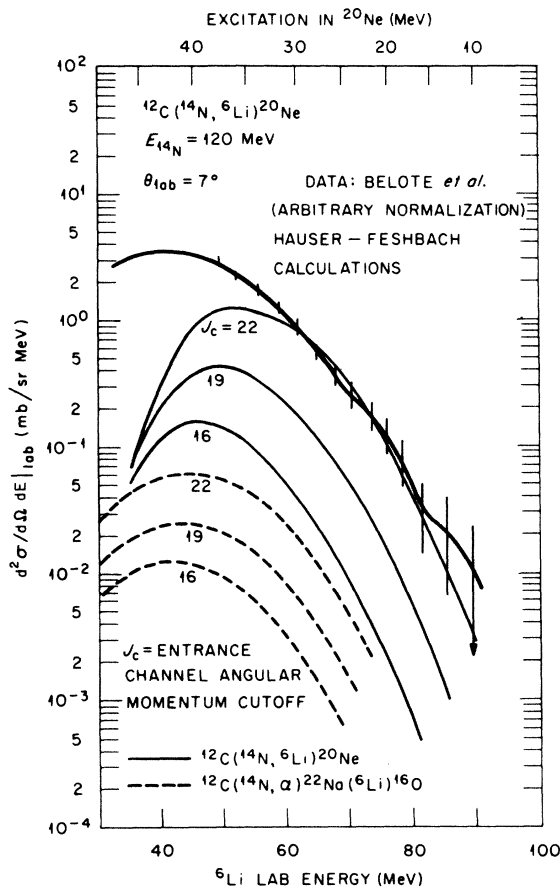


FIG. 10. Same as Fig. 8 except $E_{14\text{N}} = 120$ MeV and $\theta_{\text{lab}} = 7^\circ$. No structure corresponding to states in ${}^{20}\text{Ne}$ was apparent at this higher bombarding energy. The full curve represents a smooth fit (by eye) to the data and the vertical bars represent the uncertainties from counting statistics.

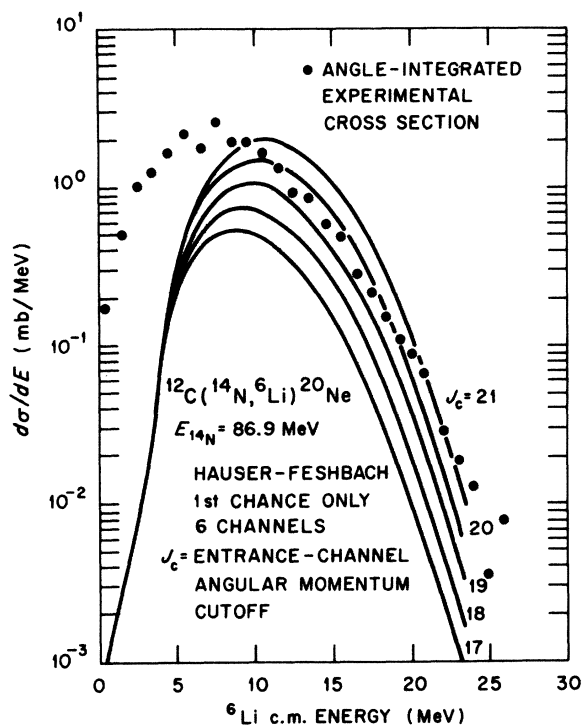


FIG. 11. Measured and predicted angle integrated yield of ${}^6\text{Li}$ as a function of the ${}^6\text{Li}$ center-of-mass energy, assuming two-body kinematics for the reaction ${}^{12}\text{C}({}^{14}\text{N}, {}^6\text{Li}){}^{20}\text{Ne}$. The normalizations of both the data and the calculations are absolute.

derpredicts the yield (see Figs. 9–11). On this basis, it appears that the production of Li and Be nuclei in the ${}^{12}\text{C} + {}^{14}\text{N}$ reaction at high energies also occurs through a direct-reaction mechanism. The direct-reaction mechanism seems to produce Li nuclei with typically lower energies than the evaporation mechanism, since ${}^6\text{Li}$ ions emitted from the compound nucleus with a center-of-mass energy equal to the Coulomb and centrifugal barrier ($l = 4$) would have, at 15° lab, an energy of ~ 34 MeV. While it is thus possible that the reaction mechanism populating low-lying states of ${}^{20}\text{Ne}$ (i.e., involving high energy ${}^6\text{Li}$ ions) is primarily compound at energies above 36 MeV c.m., the fact that the bulk of the Li yield appears to be produced by projectile fragmentation renders a statistical analysis of any portion of the spectrum suspect. Indeed a sharp division of reaction mechanisms into direct and compound processes may be artificial in this case. The experimental spectrum of ${}^6\text{Li}$ ions at high bombarding energies is not inconsistent with there being a continuous variation in re-

action process from short to long interaction times.

Thus, a statistical analysis of the magnitudes of the total Li and Be yields at energies much above 30 MeV c.m. is not valid and leads to an overestimate of the critical angular momentum. In fact, the critical angular momenta deduced from such an analysis are so large as to signal the presence of reaction mechanisms other than compound-nucleus decay. The analysis of the peak position (and not the absolute magnitude) of the yield in an Li spectrum in order to determine a critical angular momentum⁹ is not advisable as this technique would involve that portion of the data (see Figs. 9 and 10) where the contribution from nonstatistical processes is particularly large. As indicated in Figs. 10 and 11, this technique would lead to an underestimate of the critical angular momentum. The determination of critical angular momenta at high energies (and at lower energies as well) seems best done by measuring the evaporation residues.^{13–15} The measurement and analysis of light reaction products such as Li and Be provides, as shown in Fig. 6, a useful complementary method at lower bombarding energies.

V. SUMMARY

Angular distributions for the production of ${}^6,{}^7\text{Li}$ and ${}^7,{}^9\text{Be}$ in the ${}^{14}\text{N} + {}^{12}\text{C}$ reaction have been measured using ${}^{14}\text{N}$ beams of 86.9 and 157 MeV. The total yields of these nuclei are not explained by evaporation from a statistical compound nucleus. Angular distributions predicted for the energy-integrated yields differ from the observed exponential dependence on the laboratory scattering angle. Comparisons of predicted and measured energy spectra indicate that the discrepancy with the statistical model occurs mainly for particles emerging with energies near and below that of the maximum yield. The production of Li and Be nuclei with energies in this range probably proceeds via the decay of a projectile-like fragment which has been excited in a peripheral collision.

ACKNOWLEDGMENTS

We wish to thank Professor Ken Nagatani and Dr. J. Bronson, Dr. G. Nair, and Dr. H. Voit for help in acquiring the data, and Ms. K. Das for assistance with the data reduction. One of us (RGS) wishes to thank Professor T. T. Sugihara for his support of this experiment and the hospitality of the Cyclotron laboratory at Texas A & M University.

- *Work supported by the U. S. Energy Research and Development Administration under contract with the Union Carbide Corporation.
- †Present address: Babcock and Wilcox, Lynchburg, Virginia 24505.
- ‡Present address: Los Alamos Scientific Laboratory, Los Alamos, New Mexico 87545.
- ¹N. Marquardt, W. von Oertzen, and R. L. Walter, *Phys. Lett.* **35B**, 37 (1971); K. Nagatani, M. J. Levine, T. A. Belote, and A. Arima, *Phys. Rev. Lett.* **27**, 1071 (1971).
- ²R. Holub, A. F. Zeller, G. R. Choppin, R. J. DeMeijer, and H. S. Plendl, *Phys. Lett.* **43B**, 375 (1973).
- ³T. A. Belote, N. Anyas-Weiss, J. A. Becker, J. C. Cornell, P. S. Fisher, P. N. Hudson, A. Menchaca-Rocha, A. D. Panagiotou, and D. K. Scott, *Phys. Rev. Lett.* **30**, 450 (1973).
- ⁴R. Holub, A. F. Zeller, H. S. Plendl, and R. J. DeMeijer, *Nucl. Phys.* **A246**, 515 (1975).
- ⁵D. L. Hanson, R. G. Stokstad, K. A. Erb, C. Olmer, and D. A. Bromley, *Phys. Rev. C* **9**, 929 (1974).
- ⁶R. Bass, *Phys. Lett.* **47B**, 139 (1973); J. Wilczynski, *Nucl. Phys.* **A216**, 386 (1973).
- ⁷R. G. Stokstad, in *Proceedings of the International Conference on Reactions between Complex Nuclei, Nashville, Tennessee, June 1974*, edited by R. L. Robinson, F. K. McGowan, J. B. Ball, and J. H. Hamilton (North-Holland, Amsterdam/American Elsevier, New York, 1974), Vol. 2, p. 327.
- ⁸C. Volant, M. Conjeaud, S. Harar, S. M. Lee, A. Lepine, and E. F. de Silveira, *Nucl. Phys.* **A238**, 120 (1975).
- ⁹H. V. Klapdor, H. Reiss, and G. Rosner, *Phys. Letts.* **53B**, 147 (1974); **58B**, 279 (1975); H. V. Klapdor and H. Reiss, *Z. Phys.* **262**, 83 (1973).
- ¹⁰L. R. Greenwood, K. Katori, R. E. Malmin, T. H. Braid, J. C. Stoltzfus, and R. H. Siemssen, *Phys. Rev. C* **6**, 2112 (1972); Y. Eyal, I. Dostrovsky, and Z. Fraenkel, *Nucl. Phys.* **A179**, 594 (1972); J. L. C. Ford, Jr., J. Gomez del Campo, R. L. Robinson, P. H. Stelson, and S. T. Thornton, *Z. Phys.* **269**, 147 (1974); J. Gomez del Campo, J. L. C. Ford, Jr., R. L. Robinson, and P. H. Stelson, *Phys. Rev. C* **9**, 1258 (1974); A. F. Zeller, M. E. Williams-Norton, R. J. Puigh, G. E. Moore, K. W. Kemper, and G. M. Hudson, *ibid.* **14**, 2162 (1976).
- ¹¹C. Olmer, R. G. Stokstad, D. L. Hanson, K. A. Erb, M. W. Sachs, and D. A. Bromley, *Phys. Rev. C* **10**, 1722 (1974).
- ¹²M. Lowry, J. S. Schweitzer, R. Dayras, and R. G. Stokstad, *Nucl. Phys.* **A259**, 122 (1976).
- ¹³F. Fühlhofer, W. Pfeffer, B. Kohlmeyer, and W. F. W. Schneider, *Nucl. Phys.* **A244**, 329 (1975); P. Sperr, S. Vigdor, Y. Eisen, W. Henning, D. G. Kovar, T. R. Ophel, and B. Zeidman, *Phys. Rev. Lett.* **36**, 405 (1976); M. N. Nambodiri, E. T. Chulick, and J. B. Natowitz, *Nucl. Phys.* **A263**, 491 (1976); Y. Eyal, M. Beckerman, R. Chechik, Z. Fraenkel, and H. Stocker, *Phys. Rev. C* **13**, 1527 (1976); A. Weidinger, F. Busch, G. Gaul, W. Trautmann, and W. Zipper, *Nucl. Phys.* **A263**, 511 (1976).
- ¹⁴R. G. Stokstad, J. Gomez del Campo, J. A. Biggerstaff, A. H. Snell, and P. H. Stelson, *Phys. Rev. Lett.* **36**, 1529 (1976).
- ¹⁵R. G. Stokstad, R. A. Dayras, J. Gomez del Campo, P. H. Stelson, C. Olmer, and M. Zisman, *Phys. Lett.* (to be published).
- ¹⁶D. L. Hanson, Ph.D. thesis, Yale University (unpublished); and Wright Nuclear Structure Laboratory Internal Report No. 55, Yale University, 1975 (unpublished), BREAKUP—A Hauser-Feshbach Computer Code for Multistep Decay Calculations.
- ¹⁷E. T. Chulick, J. B. Natowitz, and C. Schnatterly, *Nucl. Instrum. Methods* **109**, 171 (1973).
- ¹⁸H. Feshbach, in *Nuclear Spectroscopy*, edited by F. Ajzenberg-Selove (Academic, New York, 1960).
- ¹⁹R. G. Stokstad, Wright Nuclear Structure Laboratory International Report No. 52, Yale University, 1972 (unpublished); STATIS—a Hauser-Feshbach Computer Code.
- ²⁰J. Gomez del Campo, Computer Code LILITA, 1977 (unpublished).
- ²¹M. Buenerd, C. K. Gelbke, B. G. Harvey, D. L. Hendrie, J. Mahoney, A. Menchaca-Rocha, C. Olmer, and D. K. Scott, *Phys. Rev. Lett.* **37**, 1191 (1976).